Journal of Physics: Conference Series

PAPER • **OPEN ACCESS**

Critical assessment of thermal conductivity models for Miscibility Gap Alloy-based composite Phase Change Materials for high temperature Thermal Energy Storage

To cite this article: M. Molteni *et al* 2024 *J. Phys.: Conf. Ser.* **2685** 012028

Critical assessment of thermal conductivity models for Miscibility Gap Alloy-based composite Phase Change Materials for high temperature Thermal Energy Storage

M. Molteni[1], I. M. Carraretto[2], P. Bassani[3], E. Gariboldi[1], A. Lucchini[2] and L. P. M. Colombo[2,*]

[1] Dipartimento di Meccanica, Politecnico di Milano, via Giuseppe La Masa 1, 20156 Milano (MI), Italy
[2] Dipartimento di Energia, Politecnico di Milano, via Lambruschini 4a, 20156 Milano (MI), Italy
[3] CNR-ICMATE, via Previati 1/E, 23900 Lecco (LC), Italy

* Corresponding author: luigi.colombo@polimi.it

Abstract Miscibility Gap Alloys (MGAs), such as Al-Sn-based systems, provide a viable solution for the development of composite Phase Change Materials (PCMs) for Thermal Energy Storage (TES) purposes. Their successful production depends on the cooling rate imposed to the melt. Finite Element Analyses (FEA), which relies also on thermal conductivity values, represent a powerful tool for the design of the production process. Thermal conductivity, which depends on the arrangement of the phases in the system, also affects the thermal response of the alloy. In the view of evaluating the impact of the phase morphology, the authors adapted some of the models developed for composites and solutions to Al-Sn and Al-Sn-Si-Mg alloys, characterized by broad solidification ranges in terms of composition and temperature and by significantly different phases thermal conductivity. In the fully-liquid range, Filippov and Novoselova model was selected for the description of both alloys. Models that consider sphere-like dispersions give values quite close to the theoretical upper Wiener bound when the high-melting phase is solid. The phase morphology impact is relevant when the solidification range is considered. The resulting arrangement-related thermal conductivity curves are compared to those supplied by CALPHAD-based software and to available literature data.

1. Introduction

In the last decades, Phase Change Materials (PCMs) have increasingly attracted the attention of the scientific community as a promising response to the incoming energy hunger for their capability of absorbing/releasing heat at constant temperature while undergoing phase transition. In general, the most exploited transformation is the solid-liquid one. This perspective makes PCMs very appealing for Thermal Energy Storage (TES) and Thermal Management (TEM) purposes [1]. Recently, the research has been focused on metallic PCMs [2] due to their moderate to high melting temperature, combined with high thermal conductivity and latent heat of fusion per unit volume. However, the difficulty of managing metals in the molten state, especially for their corrosivity and reactivity [3], represents a strong limitation to their use as PCMs. An approach to overcome this issue is the adoption of Miscibility Gap Alloys (MGAs) [4], i.e. systems composed of two different elements that do not interact in both solid

and liquid states [5]. Their microstructure resembles that of two-phase composites, in which the compositions of solid phases are close to the pure starting elements. The Al-Sn binary system represents a possible solution [4]. The melting onset temperature of the alloy is also close to the one of the pure Sn (232°C, highlighted by the red line in Figure 1(a)), i.e., the active PCM, and can be modified adding other elements, such as Si [6,7]. While producing the PCM material, the arrangement of phases has to be carefully controlled for the achievement of TES/TEM purposes. In particular, the active phase, i.e., PCM, which undergoes solid-liquid transition, should be well-dispersed in the thermally stable and highly thermally conductive passive phase (Figure 1(b)).

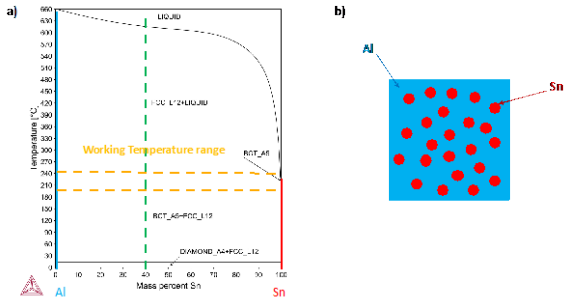

Figure 1. Al-Sn binary system showing the investigated Al-40Sn as vertical green dashed line (a) and microstructural sketch for the target MGA microstructure (b).

This microstructure could be obtained by mixing the phases in solid state [8], or by the molten metal route, if high solidification and cooling rates are considered [7,9]. In this view, the simulation of the solidification process based on Finite Element Analysis (FEA) represents a valuable tool for the correct design of these materials when produced by casting techniques. FEA simulations rely on the knowledge of the material thermophysical properties, i.e., density, specific heat capacity at constant pressure and thermal conductivity. Among them, thermal conductivity depends on the arrangement of the active phase within the matrix [10]. In addition, thermal conductivity determines the thermal response of the system. However, literature offers few data on the thermal conductivity of Al-Sn-based systems. On the other hand, the commercially available software Thermo-Calc [11] is commonly used to determine the properties of a multicomponent system, among which thermal conductivity. Its calculations rely on the CALPHAD approach, a semi-empirical approach based on experimentally obtained thermodynamic property databases. These latter allow the derivation of polynomial expressions, which describe the thermal conductivity temperature dependency. The composition influence instead, is estimated with Redlich-Kister expression [12]. It is worth mentioning that only phase arrangement-independent results are supplied by the software. Hence, the aim of this work consists in evaluating the impact of second-phase arrangement on the thermal conductivity of MGA alloys with the means of simplified analytical models. These latter were adapted from literature-granted models and developed in three different temperature-steps: fully solid, fully liquid and solidification ranges. The investigated MGA alloys are obtained by adding of 40mass% Sn to both pure Al and Al-7Si-0.4Mg alloy. The resulting systems solidify over a broad composition range and are composed of phases with different thermal conductivity. Cooling rate changes can result in a different phase-arrangement, that may lead to a consistent thermal conductivity data scatter. These latter influences both the final microstructure and the thermal response of the system. In this view, the obtained results are further compared to those directly supplied by Thermo-Calc software [11] and to available literature data.

2. Materials and methods

The study focuses on a binary Al-Sn alloy and a more complex system also containing Si and Mg. For both, the nominal mass content of Sn is 40%, as shown in Table 1, where also the reference names used in the paper are given. Figure 1 shows the presence of a namely pure Al phase (light blue line in Figure 1(a)) during and at the completion of the solidification of Al-40Sn alloy. Similarly, previous studies for

the Al-7Si-0.4Mg-40Sn, revealed that in most of the solidification range and at the end of it, there is a solid phase namely matching the chemical composition of the starting Al-7Si-0.4Mg [7]. The above situations suggested the possibility to consider Sn-bearing MGAs in their solid stage as composites made of a pure Sn and an Al/Al-7Si-0.4Mg phases. For this reason, thermal conductivity models were developed and compared on the bases of the thermal conductivity and amount/compositions of the two pure phases.

Table 1. Chemical compositions of the investigated alloys, expressed in weight percentages, simulated with Thermo-Calc.

	Al	Sn	Si	Mg	Fe	Ti
Al-40Sn	60	40	-	-	-	-
Al-7Si-0.4Mg-40Sn*	55.315	39.87	4.427	0.237	0.082	0.069

*The composition is calculated from Al-7Si-0.4Mg, considered in [13].

2.1. Thermo-Calc simulations

The thermodynamic equilibrium calculator of Thermo-Calc software [11] was adopted for the estimation of thermal conductivity, mass-normalized composition and amounts of liquid and solid phases of Sn-bearing alloys in Table 1 at temperatures from 20 to 700°C. At boundary temperatures, all of them were in fully solid and fully liquid state, respectively. A temperature step of 10°C, which automatically gets refined in proximity of phase transitions, was selected. The same has been done for Al, Sn and Al-7Si-0.4Mg to create a consistent dataset of reference phase properties to estimate the arrangement effect.

2.2. Analytical models for Sn-bearing alloys thermal conductivity

The thermal conductivity models for liquid phase (k_c) consider it as a solution. Their analytical expressions (Table 4) include the thermal conductivity of the solvent (k_1) and solutes (k_i, $i\geq2$), and the corresponding mass (atomic) fractions n_i (x_i). The solvent is considered as the phase with volume fraction ≥0.5. For the physical meaning of the models, including $\phi_{k,ij}$, y and w parameters, the reader can refer to [14] and [15].

Table 2. Models adopted for the estimation of the thermal conductivity of the liquid phase.

Model	Equation
Gas mixtures [14]	$k_c = \sum_{i=1}^{n} \frac{x_i k_i}{\sum_{j=1}^{n} x_j \phi_{k,ij}}$
Dul'nev & Zarichnyak [15]	$k_c = k_1 \left[y^2 + w(1-y)^2 + \frac{2wy(1-y)}{wy+(1-y)} \right]$
Filippov & Novoselova [15]	$k_c = k_1(1-n_2) + k_2 n_2 - 0.72(k_2 - k_1) n_2 (1-n_2)$

In the fully solid and solidification temperature ranges, when at least one of the two phases is solid, the analytical models designed for two-phases composite materials were adopted for the description of the Sn-bearing system. The models consider second phases dispersed in a matrix. The matrix is the phase with volume fraction ≥0.5. Al/Al-7Si-0.4Mg and Sn were considered for the fully solid range, whereas solid Al/Al-7Si-0.4Mg and Sn-rich liquid for the solidification range. k and v stand for the thermal conductivity [W m^{-1}K^{-1}] and the volume fraction of phases, respectively. The subscripts 1 and 2 refer to the high melting phase matrix and the second phases.

The analytical models considered for the above temperature ranges consider either a spherical dispersion or a fibre-like geometry of the same phases (Table 3). For exhaustive understanding of the former models and parameters A, B and ψ in Lewis-Nielsen model the reader is referred to [10]. The values of A, B and ψ depends on the second phases arrangement (BCC, FCC and SC for spheres and hexagonal, SC, 1D and 3D random for the fibres). The detailed explanations of models and parameters ζ and γ,

listed in Table 4, can be found in [10] and [16]. Another particular arrangement considered by analytical thermal conductivity models is the one here presented in Figure 2. The equivalent thermal network for the control volume is described by German in [17] (Figure 2).

Table 3. Models adopted in the fully solid and solidification ranges for the description of composites thermal conductivity with spherical dispersion.

Model	Equation
Maxwell [10]	$k_c = k_1\left\{1 + 3v_2\left[\left(\frac{k_2 - 2k_1}{k_2 - k_1}\right) - v_2\right]^{-1}\right\}$
Rayleigh [10]	$k_c = k_1\left\{1 + 3v_2\left[\left(\frac{k_2 - 2k_1}{k_2 - k_1}\right) - v_2 + 1.569\left(\frac{k_1 - k_2}{3k_2 - 4k_1}\right){v_2}^{10/3}\right]^{-1}\right\}$
Lewis-Nielsen [10]	$k_c = \frac{1 + AB\psi}{1 - B\psi v_2}$
Bruggeman [10]	$(1 - v_2)\frac{k_1 - k_c}{k_1 + 2k_c} + v_2\frac{k_2 - k_c}{k_2 + 2k_c} = 0$

Table 4. Models adopted in the fully solid and solidification ranges for the description of composite thermal with fibrous dispersion.

Model	Equation
Rayleigh$_{par}$ [10]	$k_{c,\parallel} = k_1\left[1 + \left(\frac{k_2 - k_1}{k_1}\right)v_2\right]$
Rayleigh$_{per}$ [10]	$k_{c,\perp} = k_1\left[1 + \frac{2v_2}{C_1 - v_2 + C_2(0.30584{v_2}^4 + 0.013363{v_2}^8)}\right]$
Halpin-Tsai [16]	$k_c = \frac{2}{3}\left(\frac{1 + \zeta\gamma v_2}{1 - \gamma v_2}\right) + \frac{1}{3}(v_2k_2 + v_1k_1)$

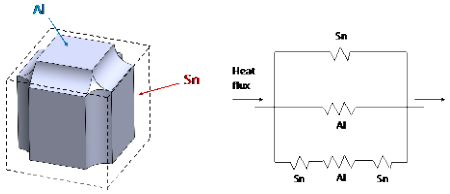

Figure 2. Sketch of the control volume and equivalent thermal resistance calculation for German model [17].

Finally, the above models are compared to the theoretical upper ($k_{c,u}$) and the lower ($k_{c,l}$) Wiener bounds for composite thermal conductivity, which corresponds to two-phase composites with second phases arranged perpendicularly or parallel to heat flux are described by eqs. (1) and (2), respectively [18]:

$$k_{c,u} = k_1v_1 + k_2v_1 \tag{1}$$

$$k_{c,l} = \frac{k_1k_2}{k_1v_2 + k_2v_1} \tag{2}$$

3. Results and discussion

3.1. Modelled thermal conductivity vs. temperature curves

The comparison among the thermal conductivity vs temperature curves of the investigated MGAs, derived from phase arrangement-related analytical models and those directly obtained by Thermo-Calc simulations, is presented and commented here with reference to the various solidification steps.

3.1.1. Fully liquid range

The comparison of thermal conductivity curves for the two alloys shown in Figure 3 suggests that predictions can significantly vary with the adopted model. Further, the thermal conductivity of the quaternary alloy, mainly differing in weight by 4.42%Si from the binary Al-40Sn, shows significant differences with respect to this latter. "Gas mixture" model provides the highest conductivities for the alloys, among the models proposed. The conductivity change induced by the presence of Si and Mg is particularly relevant for Dul'nev and Zarichnyak model, mining its reliability. The semi-empirical Filippov and Novoselova equation displays thermal conductivity curves close to those directly simulated by Thermo-Calc. Table 5 quantifies the predictions by different models with respect to simulations at the lowest and highest temperatures for fully liquid range. For these reasons, the authors adopted Filippov and Novoselova model for the description of the liquid phase in the solidification range.

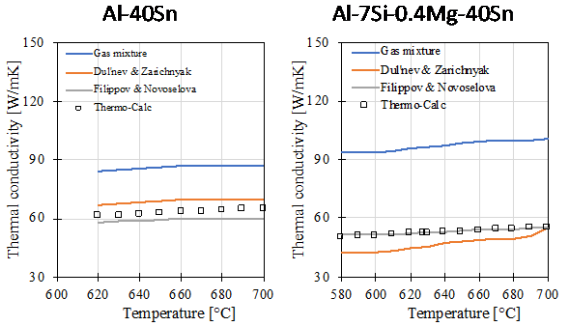

Figure 3. Thermal conductivity predicted by analytical models and by Thermo-Calc in fully liquid range.

Table 5. Percentage differences in the thermal conductivity at the lowest and highest temperatures in the fully liquid range among the models proposed and Thermo-Calc data, with respect to the latter.

Relative difference [%]	Al-40Sn liquid		Al-7Si-0.4Mg-40Sn liquid	
Model	Lowest T	Highest T	Lowest T	Highest T
Gas mixture	-37.768	-34.429	-87.222	-83.352
Dul'Nev & Zarichnyak	-10.128	-7.473	14.518	-0.235
Filippov & Novoselova	5.020	7.263	-2.477	-0.223

3.1.2. Fully solid range

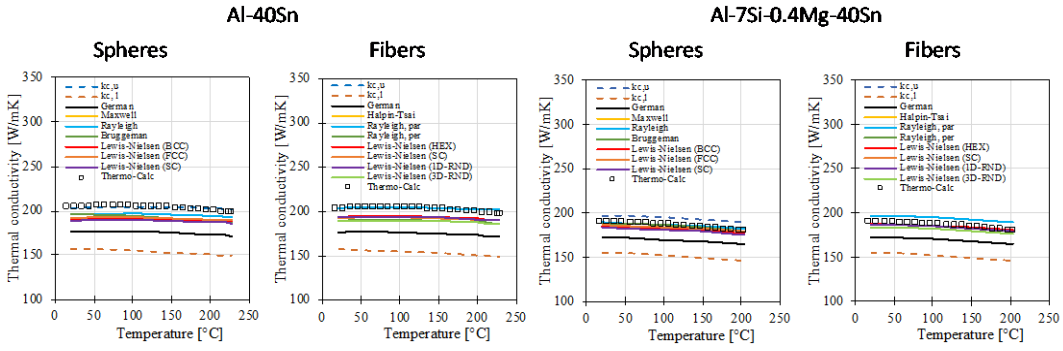

Figure 4. Thermal conductivity predicted by analytical models and Thermo-Calc in fully solid range.

In both the MGAs considered, the thermal conductivity curves predicted by most models are close to the upper Wiener bound (Figure 4), specifically the ones obtained with a spherical dispersion of second phases, described by Maxwell, Rayleigh and Bruggeman. The thermal conductivity decreases as the

dispersion arrangement changes from that of regularly arranged spheres (Lewis-Nielsen models) to the 3D arrangement of German model. The thermal conductivity data directly simulated are close to the theoretical upper Wiener bound in the case of Al-40Sn and close to spherical dispersion models for Al-7Si-0.4Mg-40Sn alloy, as quantified in Table 6. Notwithstanding the crude approximation of considering the Al-7Si-0.4Mg as a unique phase, the differences between the simulated data and spherical arrangement analytical models is lower than 4%. In general, minimal changes in the fully solid range, where phase compositions remain almost constant along the whole range, were confirmed by simulation derived curves. At least part of decrement in thermal conductivity as the temperature increases can be related to the minimal increment in solubility of Al/Mg in Sn-rich phase and vice-versa. This effect is taken into account in Thermo-Calc simulations but not in the models, simply based on the thermal conductivity of pure Sn and Al/Al-7Si-0.4Mg.

Table 6. Percentage differences in the thermal conductivity among the proposed models with respect to Thermo-Calc data at the lowest and highest temperatures of both the fully solid and solidification ranges.

Relative difference [%]	Al-40Sn solid		Al-7Si-0.4Mg-40Sn solid		Al-40Sn solidification		Al-7Si-0.4Mg-40Sn solidification	
Model	Lowest T	Highest T	Lowest T	Highest T	Lowest T	Highest T	Lowest T	Highest T
$k_{c,u}$	-0.171	-2.230	-3.211	-5.224	-0.399	4.128	-18.357	-24.577
$k_{c,l}$	22.528	24.575	18.376	18.784	47.284	4.175	7.142	-24.564
German	12.961	12.985	9.34	8.575	24.784	4.044	-8.829	-24.567
Maxwell	3.788	2.212	0.592	-1.119	6.022	4.144	-16.037	-24.573
Rayleigh	3.798	2.223	0.601	-1.109	6.042	4.144	-15.401	-24.573
Bruggeman	3.598	5.211	1.252	0.057	6.801	4.143	-16.887	-24.570
L.N. (BCC)	6.461	4.750	3.023	1.460	15.118	4.602	-11.840	-24.666
L.N. (FCC)	5.474	4.078	2.201	0.603	11.074	4.342	-13.827	-24.612
L.N. (SC)	7.295	5.622	3.814	2.283	18.964	4.872	-9.840	-24.722
Halpin-Tsai	6.571	5.392	3.256	1.788	10.920	4.151	-14.104	-24.57
$Rayleigh_{par}$	-0.171	-2.230	-3.211	-5.224	-0.399	4.129	-18.357	-24.577
$Rayleigh_{per}$	6.568	5.388	1.504	-0.196	10.911	4.151	-14.104	-24.570
L.N. (HEX)	4.769	3.316	1.531	-0.104	8.22	4.191	-15.138	-24.581
L.N. (SC)	5.083	3.648	1.829	0.206	9.789	4.242	-14.412	-24.601
L.N. (1D-RND)	4.975	3.534	1.727	0.010	11.210	4.253	-14.661	-24.594
L.N. (3D-RND)	6.936	5.610	3.590	2.041	18.241	4.849	-10.206	-24.718

3.1.3. Solidification range

The thermal conductivity vs. temperature curves shown in Figure 5 are quite spread apart, both for spherical and fibres models, suggesting a strong effect of phase arrangement. This influence is particularly evident in the intermediate temperature region, where, as the temperature decreases, the liquid phase enriches in Sn reducing its thermal conductivity. Besides, all the models predict the strong thermal conductivity reduction close to 600°C corresponding to the melting range of the Al-rich phase and the abrupt change related to Sn-rich phases solidification (200-230°C). The analytically-derived thermal conductivity curves are close to the upper bound along the whole solidification range and to the simulation-calculated up to about 350°C for Al-40Sn. At higher temperature simulated thermal conductivity values decrease more rapidly but in a smoother way than those analytically modelled. For the quaternary alloy instead, Thermo-Calc-derived curves are coherent with those derived from analytical spheres-based models along the solidification range, but they display steeper changes at its extreme portions. For both alloys, the rapid changes in the solid and the liquid compositions, possibly lead to the different trends shown in the graphs.

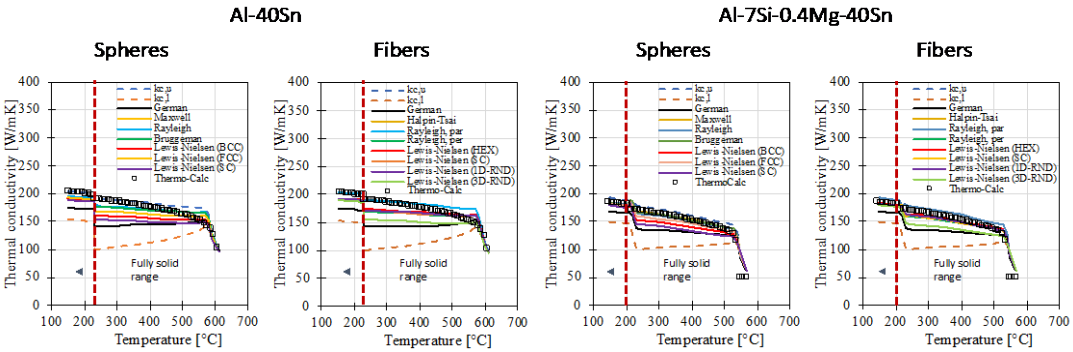

Figure 5. Thermal conductivity predicted by analytical models and Thermo-Calc in the solidification range.

3.2. Comparison with literature data

The modelled thermal conductivity curves for the Sn-containing systems, in particular those obtained by Bruggeman model and simulations, are compared to gathered literature data in order to evaluate the accuracy of the calculations. However, to the authors' best knowledge, there is a lack of experimental results regarding the investigated alloys. In the case of Al-Sn binary alloys, Meydaneri [19] investigated the thermal conductivity of a set of alloys including Al-50wt.%Sn and Al-25wt.%Sn. Their thermal conductivity well match those obtained by Li [20] by applying the Lattice Monte Carlo method to their microstructure considering the phases as pure Sn and Al. These data are presented in Figure 6(a). The best-fitting of thermal conductivity vs. Sn volume content data suggest coherent values and trends with both the Bruggeman and the Thermo-Calc curves (Figure 6). Lattice Monte Carlo method has also been applied by Rawson [18] to a Al-40Sn alloy obtained with a different production technique, leading to different microstructure. The author considered other values for the conductivity of the phases, which lead to significantly lower thermal conductivity curve (Figure 6(a)). This result highlights the importance of both the microstructure and the thermal conductivity data. No data instead was found for the quaternary Al-7Si-0.4Mg-40Sn alloy. A comparison with Al-25Sn-5Si [6] was attempted considering a mixture of 25 mass% of Sn phase and 75% of an Al-6.6%massSi phases, close Al-7Si-0.4Mg. The agreement between thermal conductivity curves of the Al-7Si-0.4Mg-40Sn and Al-25Sn-5Si alloy, displayed in Figure 6(b), was considered satisfactory. However, no indication were found in [6] regarding the temperature at which the data of solid and liquid were measured. In the graph below, they were plotted at 20°C and 600°C, respectively.

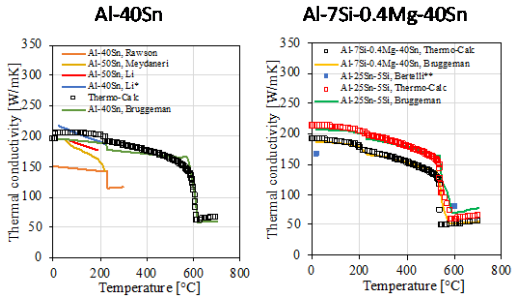

*The curve is interpolated from the data available in [20]

**The temperature related to the thermal conductivity data, here plotted at 20°C and 600°C, is not specified in [6]

Figure 6. Comparison among the experimental or modelled thermal conductivity curves for a) Al-40Sn with also data on Al-50Sn); b) Al-7Si-0.4Mg-40Sn (with also data on Al-25Sn-5Si).

4. Conclusions

This work presents a critical comparison of temperature dependent thermal conductivity data for Al/Al alloy-Sn-based MGAs. These are obtained by classical analytical models for composites/solutions combined with temperature-dependent Al, Sn, Al-7Si-0.4Mg thermal conductivity, liquid phase amount and composition derived from Thermo-Calc software. Thermal conductivity modelled data are

compared to those directly obtained from the software for the Sn-based MGAs and to available literature data in the fully solid, fully liquid and solidification ranges. The results suggest that the arrangement of the Sn/Sn-rich liquid phase is particularly important in determining the thermal conductivity, especially in the solidification range. Here, the significant liquid compositional change limits the effectiveness of the models. In particular, the models tend to diverge close to the Sn transition, a temperature range crucial for the PCM applications. The analytically derived curves with the spherical dispersion hypothesis approach the theoretical upper bound, when one of the Al-phase is solid. Moreover, these latter values are quite close with the simulation-calculated ones. Filippov and Novoselova model for solutions was adopted in the fully liquid range. The comparison with the literature is limited by the scarcity of available data, a priority for evaluating the reliability of the modelling tools considered.

5. References

[1] I Sarbu C Sebarchievici 2018 A comprehensive review of thermal energy storage *Sustain. 10*
[2] PJ Shamberger NM Bruno 2020 Review of metallic phase change materials for high heat flux transient thermal management applications *Appl Energy 258 113955.*
[3] A Rawson C Villada M Kolbe V Stahl F Kargl 2021 Suitability of aluminium copper silicon eutectic as a phase change material for thermal storage applications: Thermophysical properties and compatibility *Energy Storage. 1–15.*
[4] H Sugo E Kisi D Cuskelly 2013 Miscibility gap alloys with inverse microstructures and high thermal conductivity for high energy density thermal storage applications *Appl Therm Eng 51 1345–1350.*
[5] JZ Zhao T Ahmed HX Jiang J He Q Sun 2017 Solidification of immiscible alloys: A review *Acta Metall. Sin. (English Lett. 30) 1–28.*
[6] F Bertelli N Cheung IL Ferreira A Garcia 2016 Evaluation of thermophysical properties of Al-Sn-Si alloys based on computational thermodynamics and validation by numerical and experimental simulation of solidification *J. Chem. Thermodyn. 98 9–20.*
[7] P Bassani M Molteni E Gariboldi 2023 Microstructural features and thermal response of granulated Al and A356 alloy with relevant Sn additions *Mater. Des. 229 111879.*
[8] C Confalonieri M Perrin E Gariboldi 2020 Combined powder metallurgy routes to improve thermal and mechanical response of Al−Sn composite phase change materials *Trans. Nonferrous Met. Soc. China. 30 3226–3239.*
[9] C Confalonieri R Casati E Gariboldi 2022 Effect of Process Parameters on Laser Powder Bed Fusion of Al-Sn Miscibility Gap Alloy *Quantum Beam Sci. 6.*
[10] W. Karol 2011 A review of models for effective thermal conductivity of composite materials *J. Power Technol. 95 14–24.*
[11] Thermo-Calc Documentation Set *Thermo-Calc Version 2023a, (n.d.).*
[12] O Redlich AT Kister 1948 Algebraic Representation of Thermodynamic Properties and the Classification of Solutions *Ind. Eng. Chem. 40 345–348.*
[13] L Ceschini A Morri A Morri 2013 Effects of the delay between quenching and aging on hardness and tensile properties of A356 aluminum alloy *J. Mater. Eng. Perform. 22 200–205.*
[14] I Setiawan M Nohtomi M Katsuta 2015 Critical temperature differences of a standing wave thermoacoustic prime mover with various helium-based binary mixture working gases *J. Phys. Conf. Ser. 622.*
[15] GN Dul'nev YP Zarichnyak 1966 Thermal Conductivity of liquid mixtures *Inzhenerno-Fizicheskii Zhurnal. 11 747–750.*
[16] AJ Rawson E Kisi C Wensrich 2015 Microstructural efficiency: Structured morphologies *Int. J. Heat Mass Transf. 81 820–828.*
[17] RM German 1993 A model for the thermal properties of liquid-phase sintered composites *Metall. Trans. A. 24 1745–1752.*
[18] A Rawson E Kisi H Sugo T Fiedler 2014 Effective conductivity of Cu-Fe and Sn-Al miscibility gap alloys *Int. J. Heat Mass Transf. 77 395–405.*
[19] F Meydaneri T Buket 2016 Structural and thermo-electrical properties of Sn – Al alloys *Appl. Phys. A Mater. Sci. Process. 122:906.*
[20] Z Li C Confalonieri E Gariboldi 2021 Numerical and experimental evaluation of thermal conductivity: an application to Al-Sn alloys *Metals 2021, 11, 650.*